

Figure S1. CB1R mRNA expression in the hippocampus of R6/1 mice remains unchanged across disease progression. Quantification of *Cnr1* (CB1R) mRNA expression in the hippocampus of WT and R6/1 mice at different stages of disease progression, measured by quantitative real-time PCR (qRT-PCR). Expression levels are presented as fold change relative to WT controls at each time point. No significant differences in *Cnr1* mRNA expression were detected between genotypes at any age analyzed. Data are presented as mean \pm standard error of the mean (SEM) with n=3-4 mice per group. Statistical significance was performed using Mann-Whitney test.

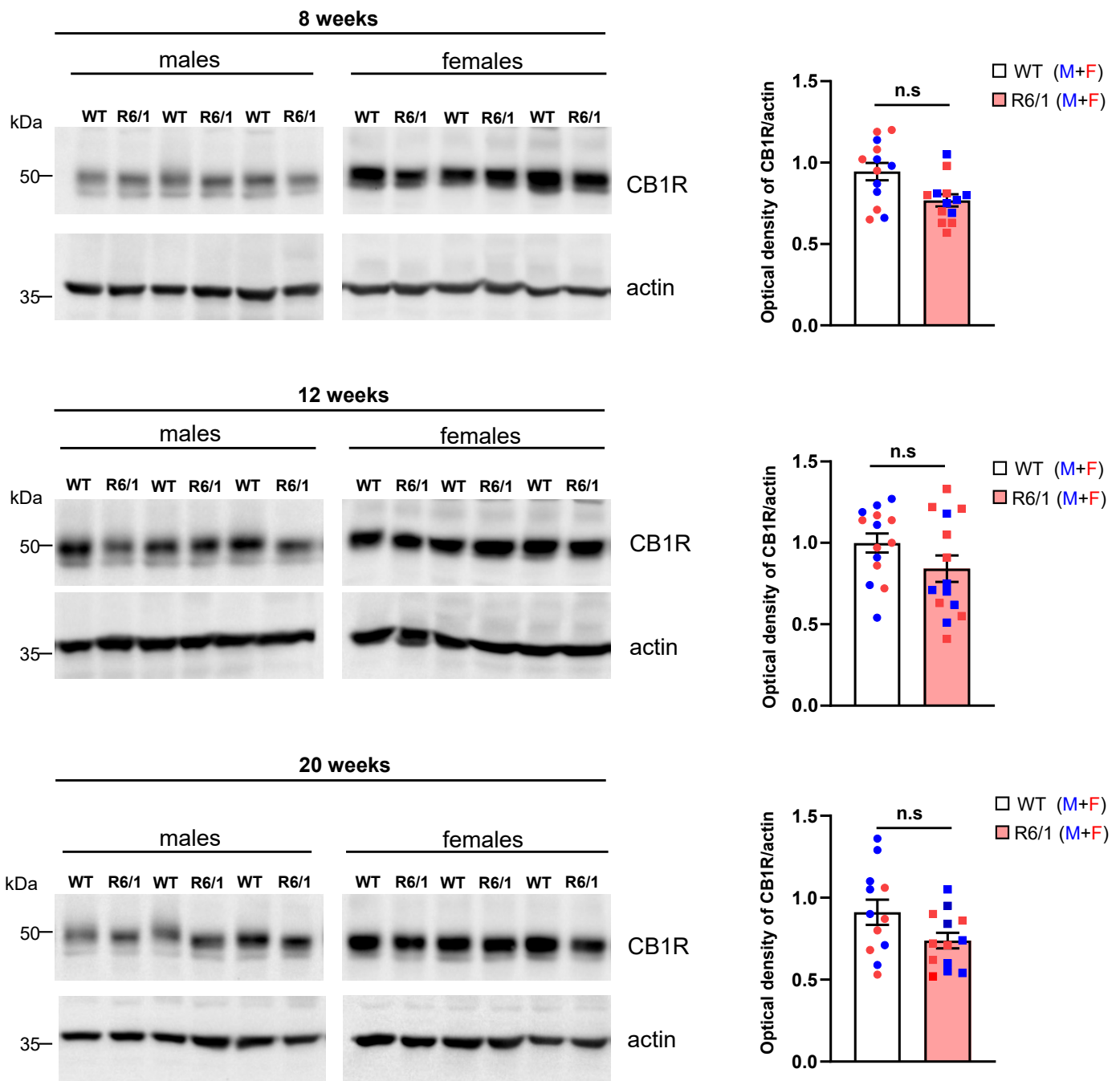
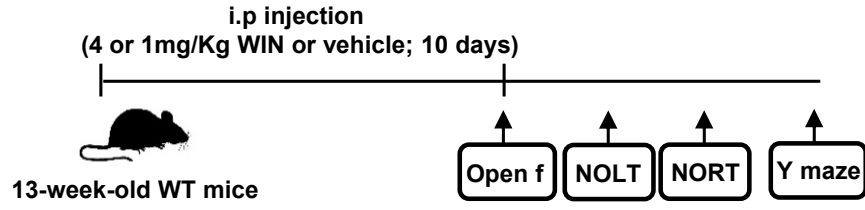


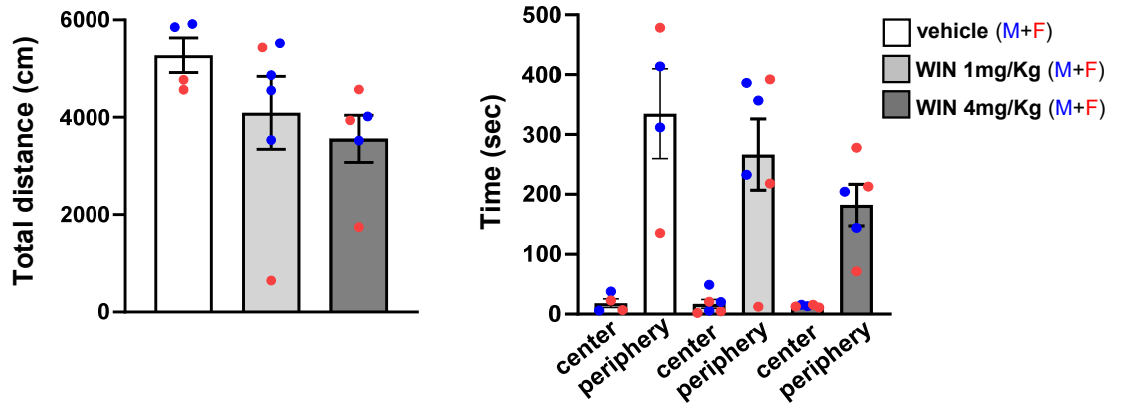
Figure S2. CB1R protein levels are not altered in the cerebellum of R6/1 mice across disease progression.

Representative immunoblots showing CB1R protein levels in total cerebellar lysates from WT and R6/1 mice at different stages of disease progression. Actin was used as a loading control. Histograms display CB1R protein levels normalized to actin (optical density). Data are presented as mean \pm standard error of the mean (SEM) with $n= 13-14$ mice per group. Statistical significance was performed using Mann-Whitney test.

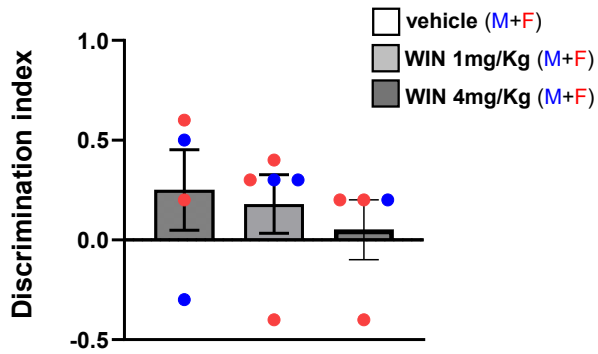
a



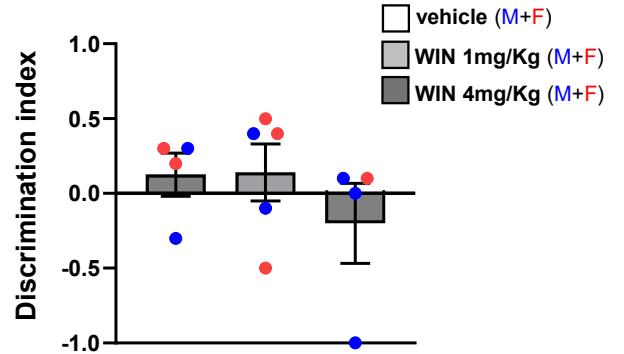
b



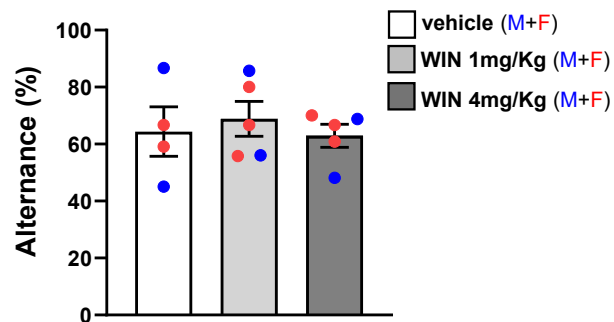
c



d



e



Supplementary Figure 3

Figure S3. Behavioral effects of WIN-55,212-2 treatment in WT mice.

a Schematic timeline showing the WIN administration protocol, followed by the sequence of behavioral tests. **b** Motor coordination and exploratory behavior assessed in the open field test, showing total distance traveled (cm) and time spent in the center versus periphery (seconds). **c** Spatial memory performance evaluated using the Novel Object Location Task (NOLT). **d** Recognition memory assessed with the Novel Object Recognition Task (NORT). **e** Spatial working memory assessed by the Y-maze test. Statistical analysis was performed using one-way ANOVA. Data are presented as mean \pm standard error of the mean (SEM) with n=4-6 mice per group.

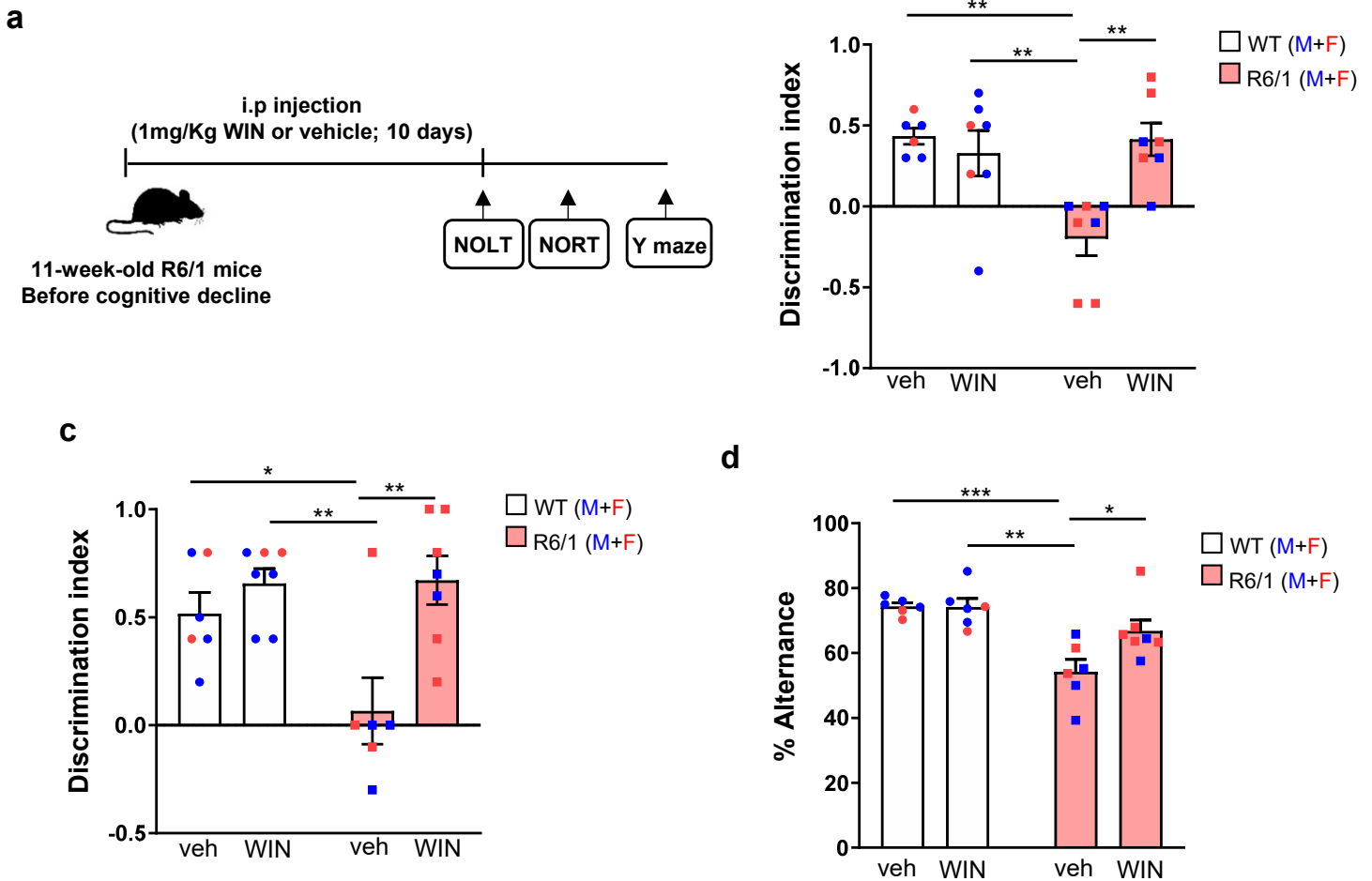


Figure S4. Sub-chronic WIN-55,212-2 treatment in R6/1 mice at presymptomatic stages prevents memory deficits.

a Schematic timeline showing the WIN administration protocol, followed by the sequence of behavioral tests. **b** Performance in the Novel Object Location Task (NOLT), assessing spatial memory. Two-way ANOVA revealed significant effects of WIN treatment ($F(1,36) = 6.785$, $p = 0.0133$) and genotype ($F(1, 36) = 4.918$, $p = 0.033$). **c** Performance in the Novel Object Recognition Task (NORT). Two-way ANOVA revealed a significant effect of WIN treatment ($F(1,22) = 1.39$, $p = 0.0027$). **d** Performance in the Y-maze task, assessing working spatial memory. Two-way ANOVA revealed significant effects of WIN treatment ($F(1,21) = 4.479$, $p = 0.0464$) and genotype ($F(1, 21) = 22.02$, $p = 0.0001$). Data are presented as mean \pm standard error of the mean (SEM) with $n = 8-12$ animals per group and genotype. Post hoc comparisons using Tukey's test indicated $*p < 0.05$, $**p < 0.01$ and $***p < 0.001$.

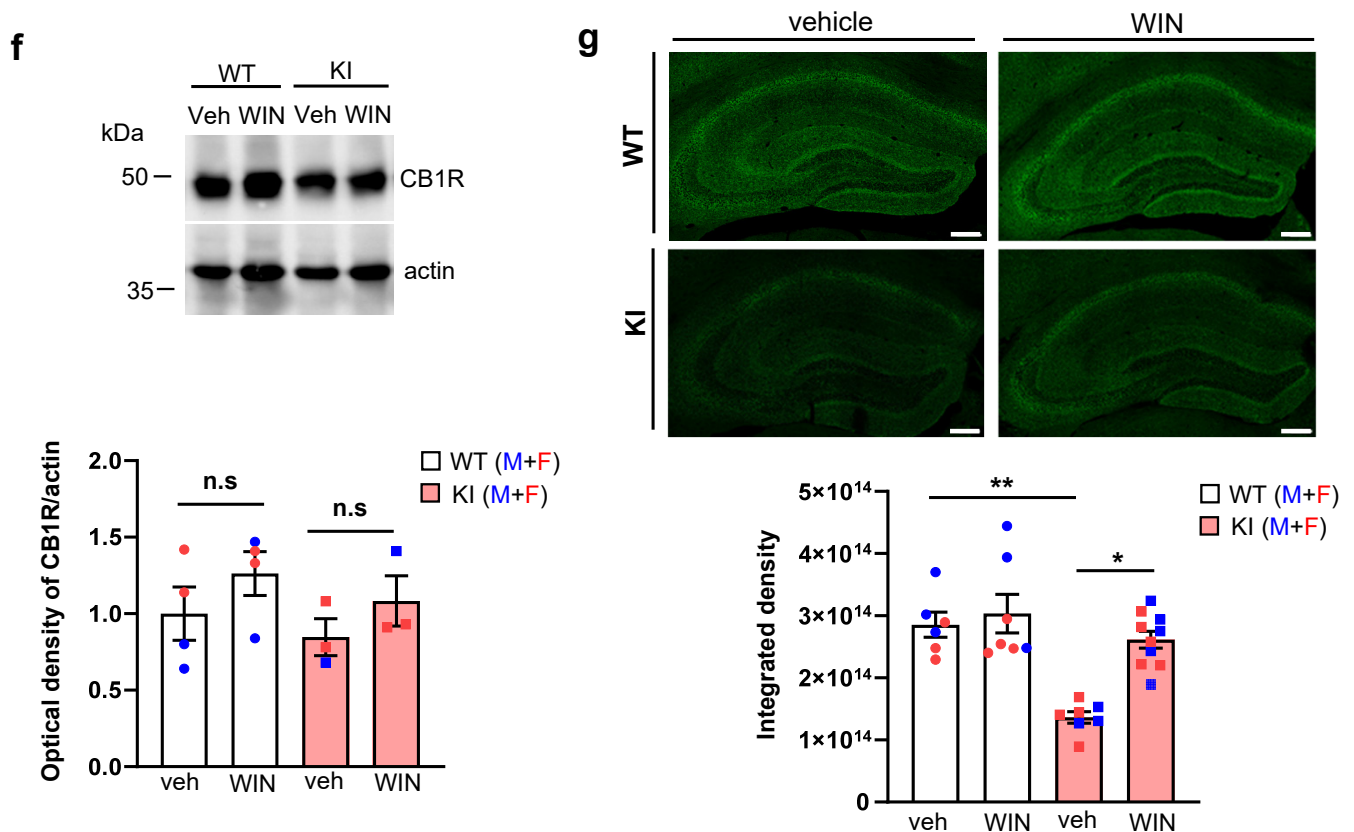
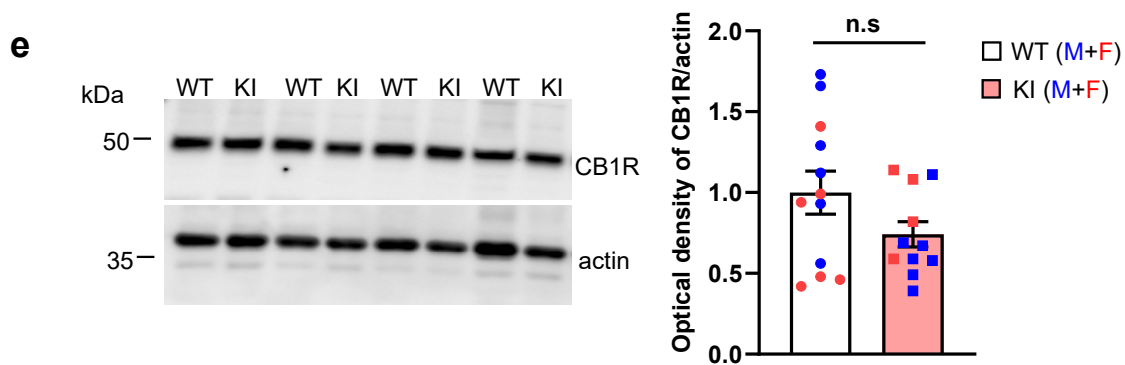
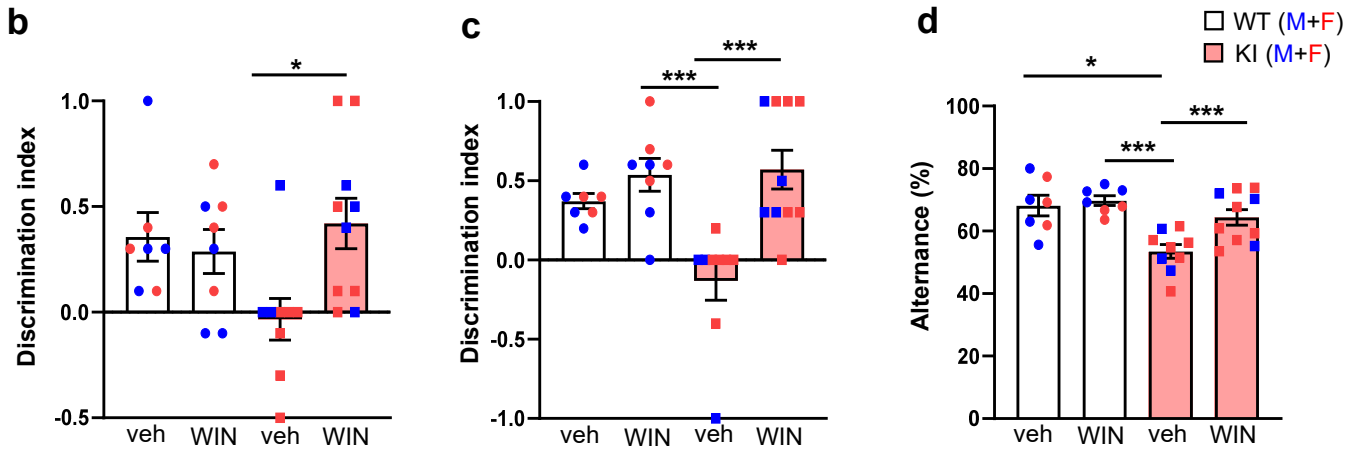
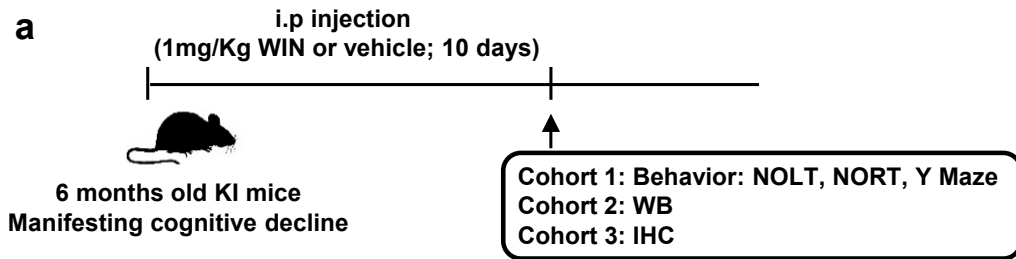


Figure S5. Sub-chronic WIN-55,212-2 treatment improves memory performance and restores hippocampal CB1R expression in symptomatic Hdh^{Q7/Q111} mice.

a Schematic timeline showing the WIN administration protocol, followed by the sequence of behavioral tests and biochemical analyses. **b** Spatial memory performance assessed using the Novel Object Location Task (NOLT). Two-way ANOVA revealed significant effects of WIN treatment ($F(1,62)=8.541$, $p=0.0048$) and genotype ($F(1,62)=28.44$ $p<0.0001$). **c**. Recognition memory assessed using the Novel Object Recognition Task (NORT). Two-way ANOVA revealed significant effects of WIN treatment ($F(1,30) =15.30$, $p=0.0005$) and genotype ($F(1,30) =4.515$ $p=0.0420$). **d**. Spatial working memory performance assessed using the Y-maze test. Two-way ANOVA revealed significant effects of WIN treatment ($F(1,29) =6.161$, $p=0.0191$) and genotype ($F(1,29) =15.93$, $p=0.0004$). Data are presented as mean \pm standard error of the mean (SEM) with $n=6-10$ mice per group. Tukey's post hoc test indicated $*p<0.05$ and $***p<0.001$. **e**. Representative immunoblots showing CB1R protein levels in total hippocampal lysates from naive Hdh^{Q7/Q7} (WT) and Hdh^{Q7/Q111} (KI) mice at 6 months of age. Actin was used as a loading control. Histogram shows CB1R levels normalized to actin (optical density). Data are presented as mean \pm standard error of the mean (SEM) with $n= 11-12$ mice per group. Statistical significance was performed using Mann-Whitney test. **f**. Representative immunoblots of CB1R in hippocampal lysates from vehicle-and-WIN-treated Hdh^{Q7/Q7} (WT) and Hdh^{Q7/Q111} (KI) mice. Actin was used as a loading control. Histogram shows CB1R levels normalized to actin (optical density). Data are presented as mean \pm standard error of the mean (SEM) with $n= 3-4$ mice per group and genotype. **g**. Representative confocal images showing CB1R immunofluorescence in hippocampal coronal sections from vehicle or WIN-treated Hdh^{Q7/Q7} (WT) and Hdh^{Q7/Q111} (KI) mice. Scale bar = 100 μ m. Data are presented as the mean \pm standard error of the mean (SEM) with $n = 6-10$ mice per group and genotype. Two-way ANOVA revealed significant effects of WIN treatment ($F(1,30) =12.05$, $p=0.0016$) and genotype ($F(1,30) =8.322$ $p=0.0072$). Tukey's post hoc test indicated $*p<0.05$ and $**p<0.01$.

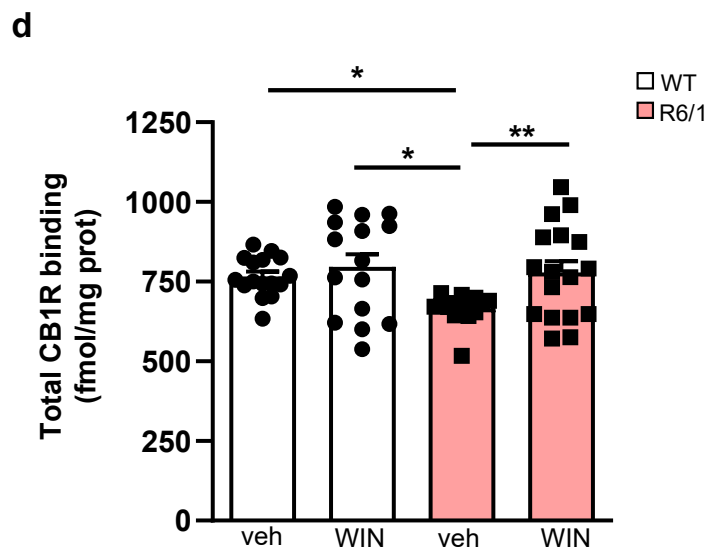
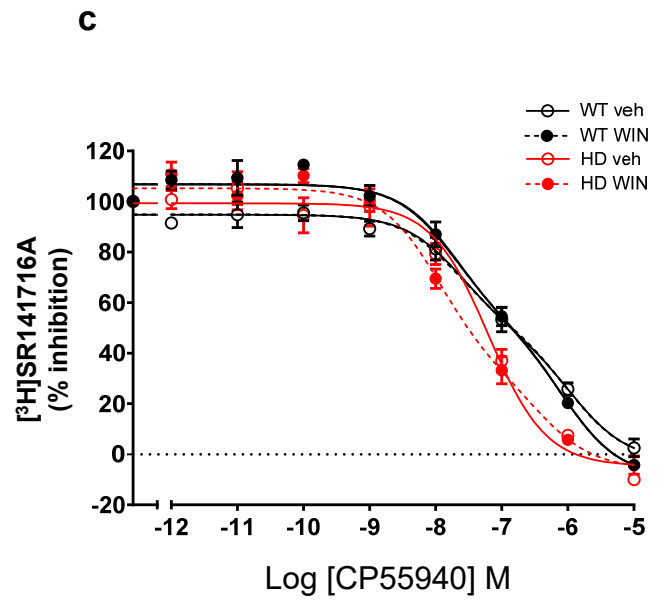
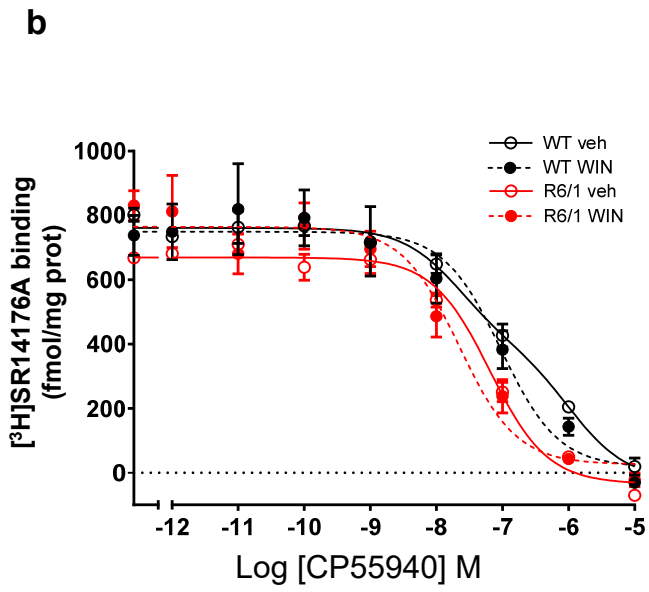
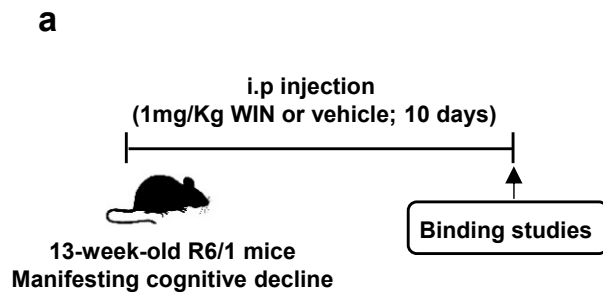


Figure S6. Sub-chronic WIN-55,212-2 treatment restores CB1R binding affinity.

a Schematic timeline showing the WIN administration protocol, followed by the CB1R binding analysis. **b** [³H] SR141716A binding assays inhibition curves by CP55,940 (fmol/mg protein) in hippocampal membrane homogenates from vehicle-treated WT mice (n = 14), WIN-treated WT mice (n = 10), vehicle-treated R6/1 mice (n = 10) and WIN-treated R6/1 mice (n = 9). Statistical analysis using an F-test revealed significant differences between groups (p < 0.001). **c** Percentage of [³H]SR141716A binding inhibited by CP55,940. Significant differences in IC₅₀ values and best-fit models (one or two binding sites) were observed between groups, with an F-test indicating statistical significance (p < 0.001). **d**. Total binding of [³H]SR141716A, measured under conditions corresponding to the maximum binding (B_{max}), reflects CB1R density and is expressed as fmol/mg of protein. Data are presented as mean ± standard error of the mean (SEM) (n = 4-6 mice per group and genotype). Two-way ANOVA revealed a significant effect of WIN treatment (F(1,60) = 7.188, p = 0.0095) and genotype (F(1,60) = 5.313, p = 0.0246). Post hoc comparisons using Tukey's test indicated *p < 0.05, **p < 0.01.

Figure S7. Hippocampal CB2R expression is unaltered in naive or WIN-55,212-2-treated HD mice.

Representative immunoblots showing CB2R levels in total hippocampal lysates from naive WT and R6/1 mice at 12 weeks of age (**a**) and Hdh^{Q7/Q7} (WT) and Hdh^{Q7/Q111}(KI) mice at 6 months of age (**b**). Actin was used as a loading control. Histograms show CB2R protein levels normalized to actin (optical density). Data are presented as the mean \pm standard error of the mean (SEM) with n= 12-13 mice per group. Statistical significance was determined by the Mann-Whitney test. **c and d.** Schematic timeline showing the WIN administration protocol, followed by the subsequent biochemical assays. Representative immunoblots showing CB2R levels in total hippocampal lysates from vehicle and WIN-treated WT and R6/1 mice (**c**) and Hdh^{Q7/Q7} (WT) and Hdh^{Q7/Q111} (KI) mice (**d**). Actin was used as a loading control. Histograms show CB2R protein levels normalized to actin (optical density). Data are presented as the mean \pm standard error of the mean (SEM) with n= 3-4 mice per group and genotype. Statistical significance was assessed by Mann-Whitney test.

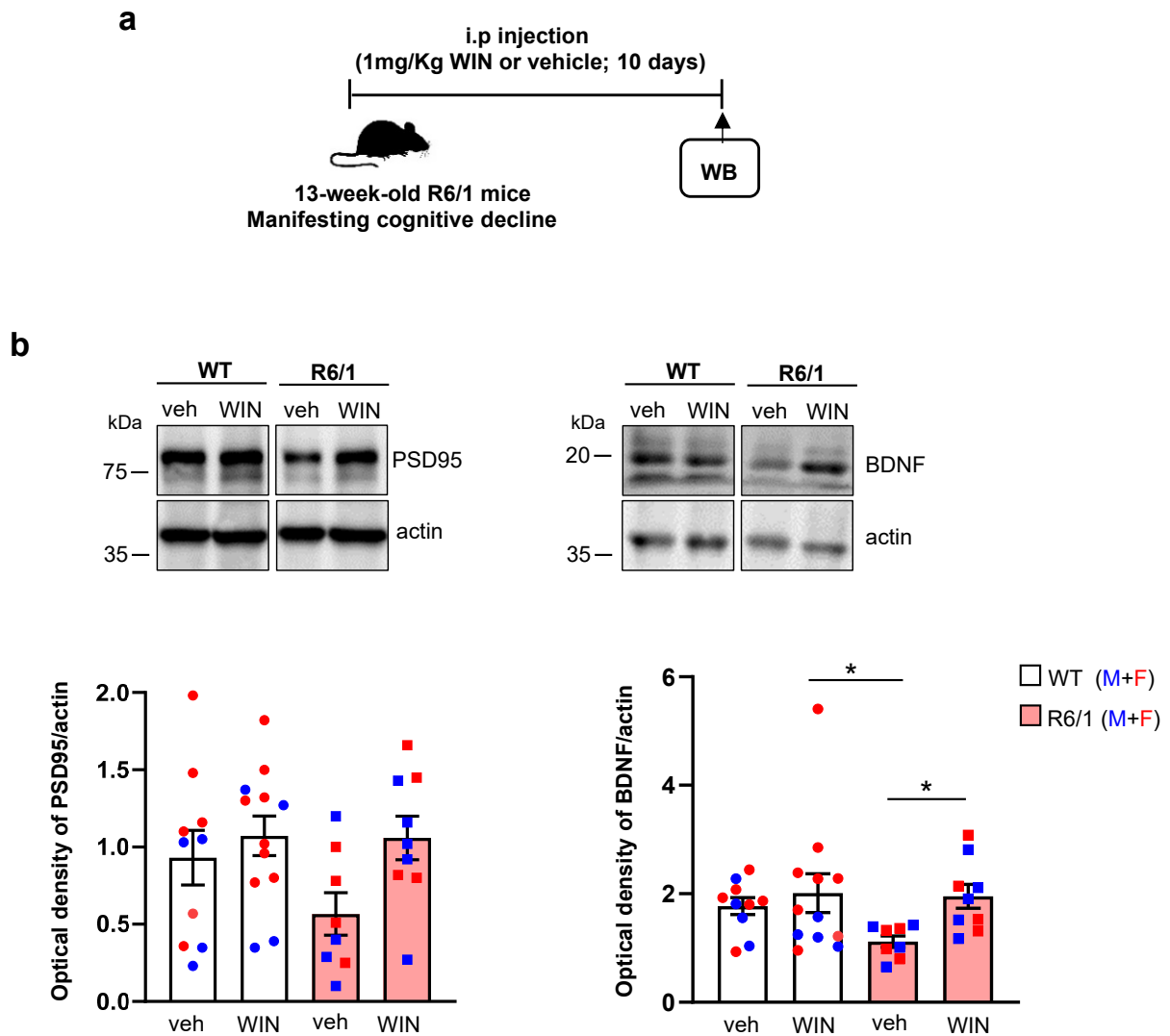


Figure S8. Sub-chronic WIN-55,212-2 treatment recovers the expression of synaptic-related proteins in R6/1 mice.

a Schematic timeline showing the WIN administration protocol, followed by the sequence of biochemical analyses. **b**

Representative immunoblots showing the levels of PSD95 and BDNF in total hippocampal lysates from vehicle-and-WIN-treated WT and R6/1 mice. Actin was used as a loading control.

Histograms show PSD95 and BDNF protein levels normalized to actin (optical density). Data are presented as the mean \pm standard error of the mean (SEM) with $n = 8-12$ mice per group. Statistical analysis was performed using two-way ANOVA, revealing significant effects of WIN treatment on PSD95 (WIN effect $F(1,33) = 4.481$, $p = 0.04$) and BDNF (WIN effect $F(1,33) = 6.568$, $p = 0.0151$). Tukey's pots hoc test indicated $*p < 0.05$.

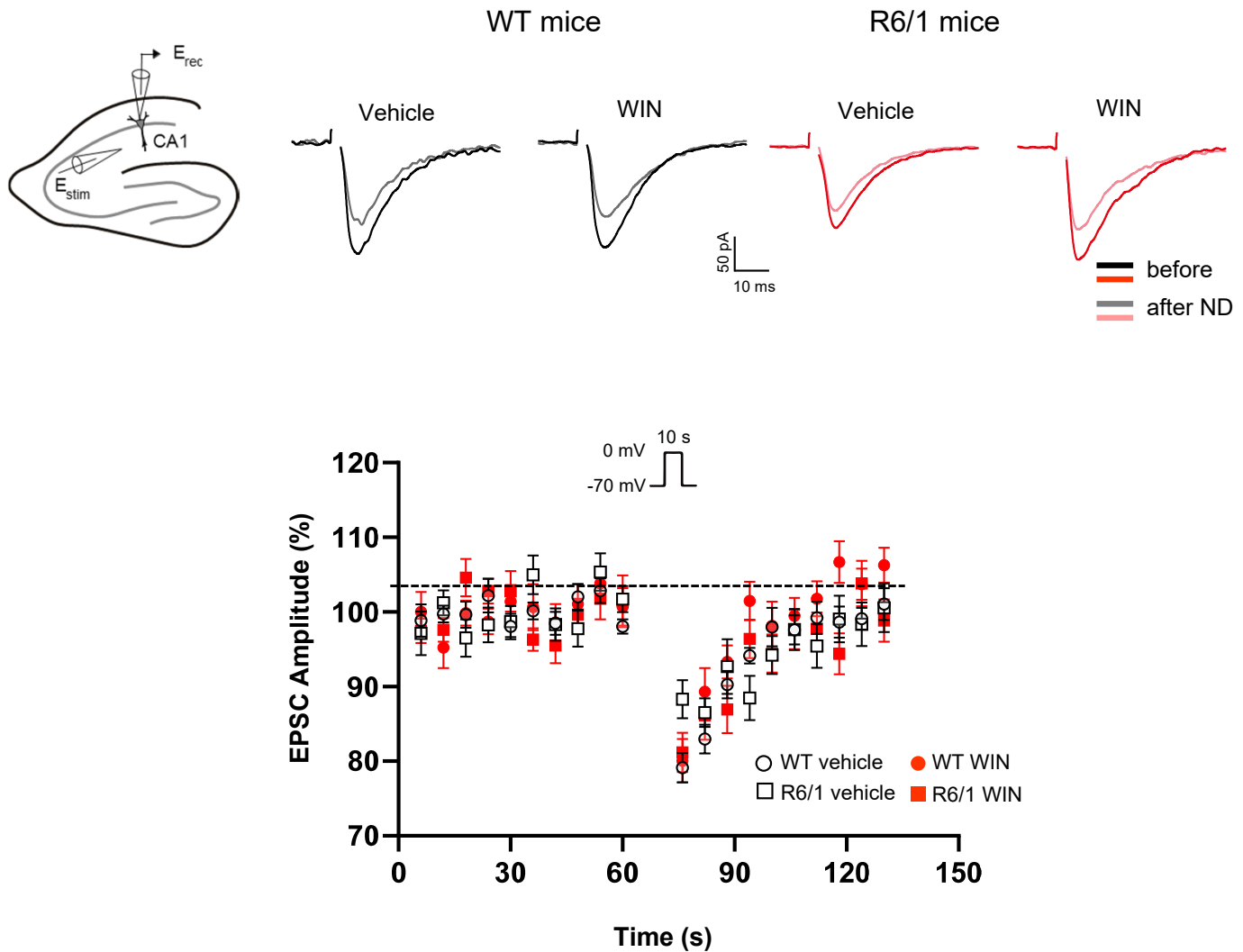


Figure S9. Depolarization-induced suppression of excitation (DSE) is not altered in the hippocampus of R6/1 mice.

Representative traces of excitatory postsynaptic currents (EPSCs), averaged from two responses, recorded from CA1 pyramidal neurons before (pre) and after (post) a 10-second depolarizing step to 0 mV, illustrating DSE under different experimental conditions. Normalized average EPSC amplitude before and after depolarization are shown for the following experimental conditions: vehicle-treated WT (n=12 neurons, 6 mice), vehicle-treated R6/1 (n= 14 neurons, 6 mice), WIN-treated (n= 10 neurons, 4 mice), and WIN-treated R6/1 (n= 20 neurons, 5 mice). Data are presented as mean \pm standard error of the mean (SEM). Statistical significance was determined using two-way ANOVA with Bonferroni post-hoc test. Both male and female mice were included in all analysis.

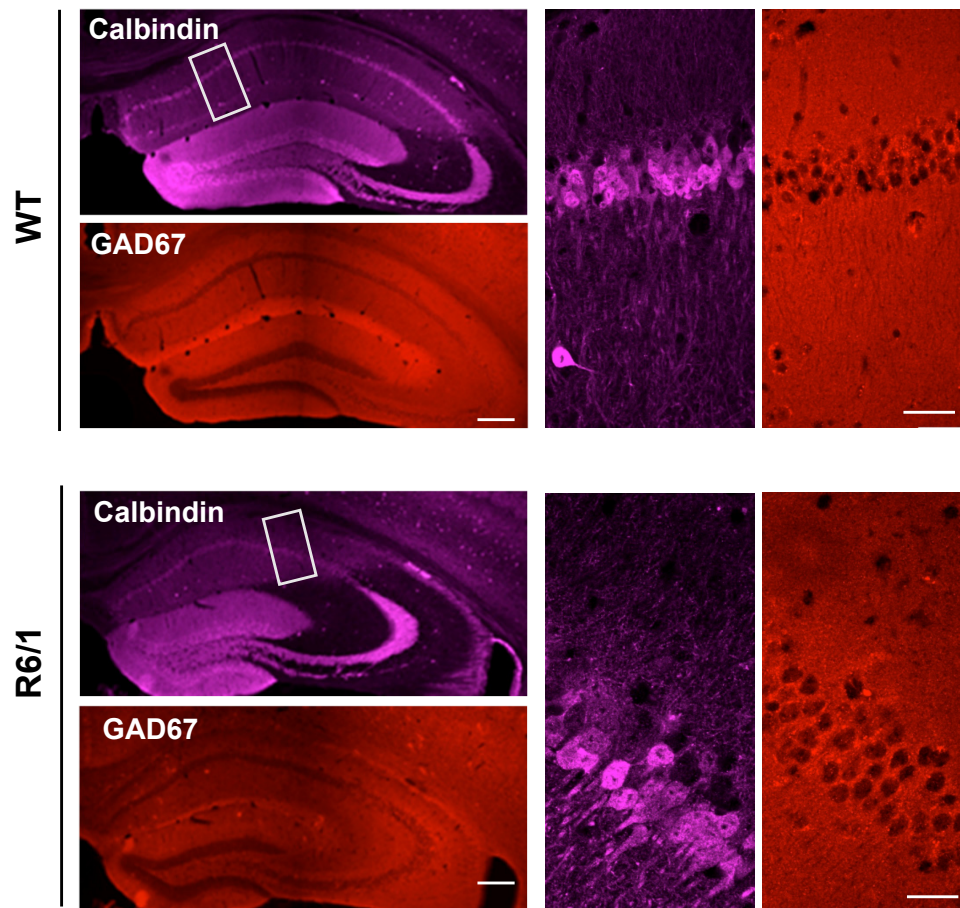
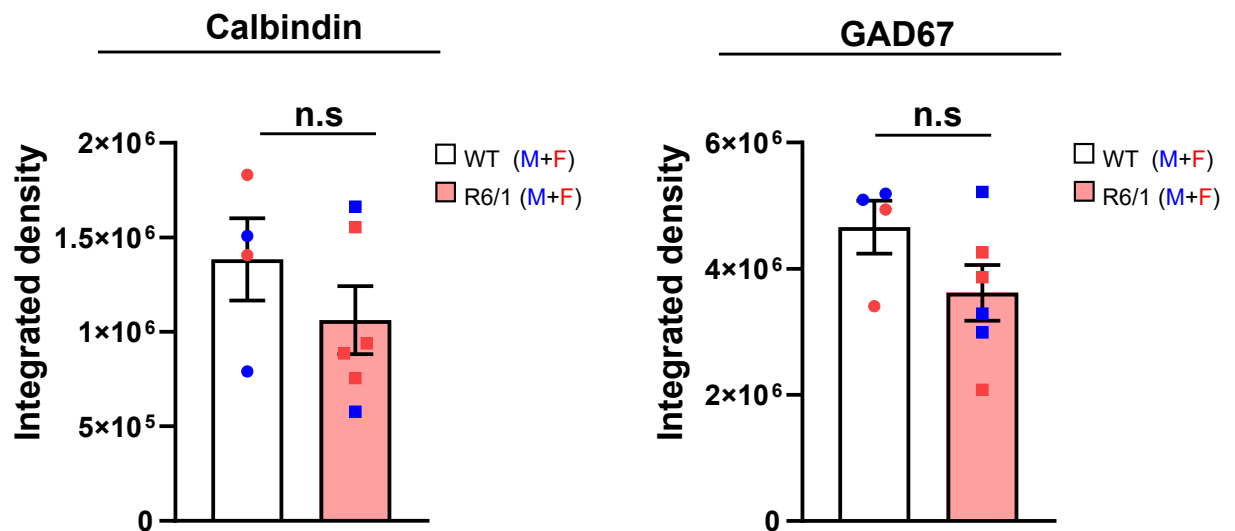
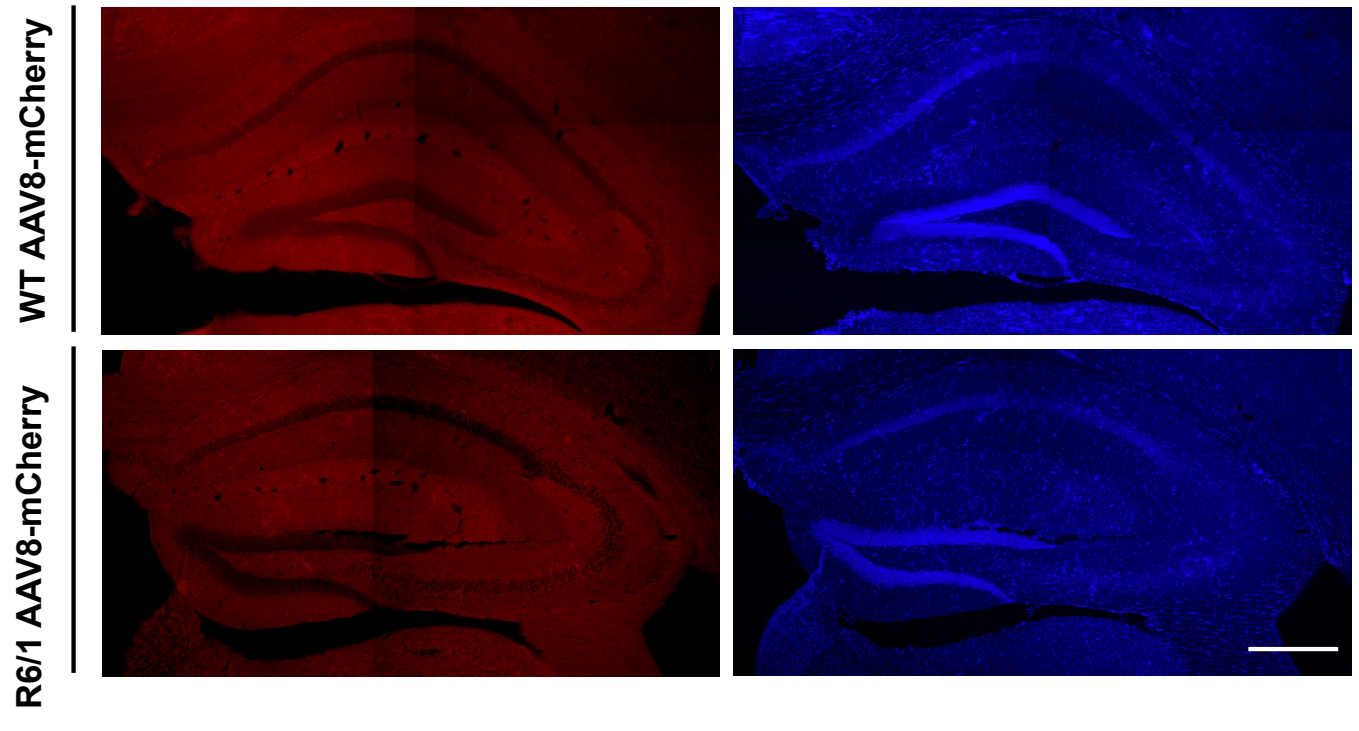
a**b**

Figure S10. Characterization of calbindin and GAD67 expression in the hippocampus of WT and R6/1 mice. **a** Representative confocal images at low and high magnification showing the distribution of calbindin (purple) and GAD67 (red) in the hippocampus of naive WT and R6/1 mice. Scale bar = 200 μ m (low magnification) and 25 μ m (high magnification). Histograms display the integrated density of calbindin and GAD67 immunoreactivity. Data are presented as the mean \pm standard error of the mean (SEM) with $n = 4-6$ mice per group. Statistical significance was assessed using the Mann-Whitney test.

a



b

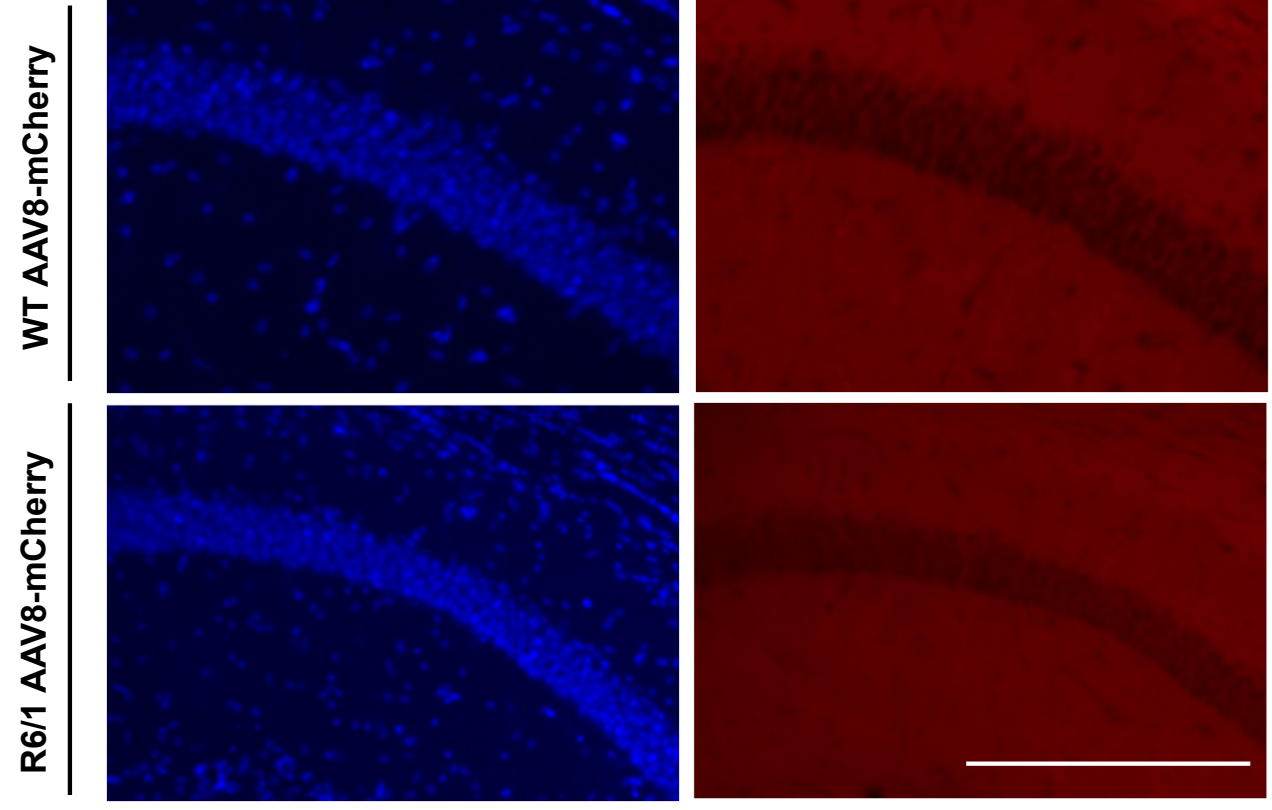


Figure S11. Characterization of AAV8-mCherry transduction in the hippocampus of WT and R6/1 mice.

Representative confocal images showing AAV8-mediated mCherry transduction in the hippocampus of 13-week-old WT and R6/1 mice. Panel (a) displays low magnification images while panel (b) shows high magnification images highlighting the diffuse distribution of mCherry fluorescence in both genotypes. The images illustrate comparable transduction efficiency between WT and R6/1 mice. Scale bar are provided for each magnification (Scale bar=250 μ m).